Percolation, quantum tunnelling and the integer Hall effect

1988 J. Phys. C: Solid State Phys. 21 2665

(http://iopscience.iop.org/0022-3719/21/14/008)

J. Phys. C: Solid State Phys. **21** (1988) 2665–2679. Printed in the UK

Percolation, quantum tunnelling and the integer Hall effect

J T Chalker and P D Coddington
Physics Department, Southampton University, Southampton SO9 5NH, UK

Received 16 October 1987

Abstract. A model is introduced for Anderson localisation in the integer quantum Hall regime. The model represents a system with a disordered potential that varies slowly on the scale of the magnetic length, but includes quantum tunnelling and interference effects. Numerical calculations indicate that the localisation length diverges only at the centre of each Landau band. The scaling behaviour near the mobility edge is analysed: results suggest that quantum tunnelling induces crossover at the classical percolation threshold to critical behaviour similar to that found previously for a rapidly varying potential.

1. Introduction

There is an intuitively appealing picture of Anderson localisation in the context of the integer quantum Hall effect which relates localisation to classical percolation. The relevant ideas have been developed by a number of authors: Tsukada (1976), Iordansky (1982), Kazarinov and Luryi (1982), Ono (1982), Prange and Joynt (1982), Trugman (1983), Shapiro (1986) and Wilkinson (1987). Their starting point is to consider a system of non-interacting electrons moving in a two-dimensional disordered potential, $V(\boldsymbol{r})$, which varies on a length scale, λ, that is much larger than the magnetic length, l_c. In this limit there are two components to electron motion which have widely separated timescales: rapid cyclotron orbiting, with frequency ω_c, and slow drift of the orbit guiding centre. The essential simplifying feature is that guiding centres drift along equipotentials (or contours) of $V(\boldsymbol{r})$ (Prange and Joynt 1982). From this it is argued that each eigenstate has its probability density concentrated on a strip of width l_c around one (connected) contour of $V(\boldsymbol{r})$. The energy of an eigenstate is the sum of the kinetic energy of cyclotron motion, $(n+\frac{1}{2})\hbar\omega_c$ (where $n = 0, 1, 2, \ldots$ labels the Landau band), and the potential energy of the contour with which the state is associated. By this reasoning, there are extended eigenstates at the energy $(n+\frac{1}{2})\hbar\omega_c + V_0$ if the equipotentials of $V(\boldsymbol{r})$ at energy V_0 percolate; otherwise all eigenstates at this energy are localised. Unless an external electric field is present, it is expected very generally that equipotentials of $V(\boldsymbol{r})$ percolate only at one energy; hence extended eigenstates are found at a unique energy within each disorder-broadened Landau band.

The reliability of this picture has been examined in detail by Trugman (1983). The only important omission (if $\lambda/l_c \gg 1$) is the neglect of electron tunnelling between separate contours at the same potential that come close together (on the scale l_c), which happens near saddle points of the potential. Trugman showed that, at any fixed energy

0022-3719/88/142665 + 15 $02.50

not equal to the percolation energy of a Landau band, the localised eigenstates are stable against inclusion of tunnelling for sufficiently large λ/l_c. His arguments also indicate, however, that for any fixed value of λ/l_c, tunnelling may be significant for eigenstates with energies in a range around each percolation energy. This energy range narrows as λ/l_c increases but always includes the eigenenergies of any extended states in the system. Since the existence of extended states is a particularly interesting and mysterious aspect of the integer quantum Hall effect, failure of the classical picture at these energies is especially significant. In principle, tunnelling might produce bands of extended states with finite energy width; equally, one can ask why quantum interference between waves that follow different tunnelling paths does not localise all states.

In this paper we introduce a model which makes use of the simplifying features of a slowly varying potential but incorporates fully quantum tunnelling and interference effects. The model, which is described in detail in the following section, represents electron wave propagation on a random network. The links of the network correspond to pieces of contour that are far (on the scale l_c) from any other section of contour at the same energy. The nodes of the network correspond to regions where two pieces of contour at the same potential come close together. Each link transmits waves only in one direction, the direction of drift for guiding centres on the corresponding piece of contour, and has a phase associated with it, which is the phase difference for a wavefunction between the two ends of the corresponding piece of contour. Randomness enters the model through a random choice for these phases. Each node has a scattering matrix associated with it, which contains the amplitudes for electron transitions between incoming and outgoing links. Unitarity restricts the scattering matrices to (essentially) a one-parameter family; variation of this parameter through its range corresponds to varying the Fermi energy across a Landau band in the physical system.

We study the model numerically, using a standard technique to calculate the decay length for the transmission matrix of long, narrow cylinders (Pichard and Sarma 1981, MacKinnon and Kramer 1981, 1983) which is identified with the localisation length (Johnston and Kunz 1983). Finite-size scaling is employed to extrapolate these results and obtain the localisation length in an infinite system.

It is remarkable that although the network model appears to be only a crude caricature of the original physical system, its behaviour contains the features necessary for a qualitative understanding of the integer quantum Hall effect (von Klitzing *et al* 1980, von Klitzing 1986): localised states in the Landau band tails and extended states in the band centre, probably existing only at one energy. To this degree, the classical picture survives the inclusion of quantum tunnelling. There are, however, quantitative changes. In the classical picture, the localisation length diverges with an exponent $\nu = \frac{4}{3}$ (Trugman 1983, and references therein). For the network model we find a different value, $\nu = 2.5 \pm 0.5$, which, interestingly, is in reasonable agreement with two estimates for a rapidly varying potential ($\lambda/l_c = 0$): $\nu \geq 2$ (Aoki and Ando 1985) and $\nu = 1.9 \pm 0.2$ (Hikami 1986). If correlations at the critical point of the model are conformally invariant (Cardy 1984, 1987), then we find that eigenfunctions at this energy decay with a power law: $|\psi(\boldsymbol{r})\psi(\boldsymbol{r}')| \sim |\boldsymbol{r} - \boldsymbol{r}'|^{-\eta}$ where $\eta = 0.269 \pm 0.003$.

The stability against quantum tunnelling of the qualitative feature of the classical picture, that eigenfunctions are extended at only one energy, may be specific to two dimensions. A version of the network model defined on a Cayley tree has bands of extended states (Chalker and Siak 1988).

There have been two previous studies of localisation in the quantum Hall regime using finite-size scaling (Schweitzer *et al* 1984, Aoki and Ando 1985) which treat the

opposite limit to the one considered here: that of a rapidly varying potential ($\lambda/l_c = 0$). In the former, a lattice model was examined, with the magnetic field represented by phase factors in the hopping matrix elements; in the latter, a continuum system was discretised by projecting onto the lowest Landau level. The effect of a slowly varying potential has been studied in the lowest Landau level by Ando and Aoki (1985). The scaling behaviour of the network model appears to be considerably simpler than in these systems.

Wave propagation on networks has been discussed in other contexts (see, for example, de Gennes 1981, Shapiro 1982, Avron *et al* 1987). The main distinction between the present model and earlier ones is that waves propagate in only one direction on the links of our model, which is a consequence of the absence of time-reversal invariance due to the magnetic field.

The remainder of this paper is organised as follows. The motivation for the network model is explained in the following section and a formal definition given; the relationship with some other approaches is also discussed. In § 3, results of numerical calculations are presented and interpreted. In the final section our conclusions are summarised briefly.

2. The network model

To explain the motivation for the network model, we discuss first the problem of finding an eigenstate of the Schrödinger equation for an electron (of mass m and charge e) moving in the x–y plane with a potential $V(x, y)$ and a uniform, perpendicular magnetic field of strength B. The potential will be assumed slowly varying in the sense $|\nabla V(x, y)| \ll \hbar\omega_c/l_c$, where $\hbar\omega_c = \hbar|e|B/m$ and $l_c^2 = \hbar/|e|B$, although Prange and Joynt (1982) and Shapiro (1986) have discussed circumstances under which this assumption might be relaxed.

Suppose that the boundary conditions admit an eigenstate of energy $E = (n + \frac{1}{2})\hbar\omega_c + V_0$. Solution of the Schrödinger equation can be accomplished in two steps if the system is divided into a number of small regions. The first step is to integrate the equation within each region, for energy E; the second is to match solutions obtained in different regions along common boundaries.

To be specific, consider the potential sketched in figure 1. Portions of contour at potential V_0 (heavy curve) are enclosed in a number of strips and circles (broken curves) of dimensions $\gg l_c$, which will correspond to the links and nodes of our network model. The eigenfunction sought has negligible amplitude outside these broken boxes.

The solution within one strip can be written following Trugman (1983), after introducing curvilinear coordinates, s and t, locally parallel and perpendicular, respectively, to the equipotentials. The full functional form of this solution, $\psi(s, t)$, contains a great deal of redundant information and is conveniently replaced with a complex function of one variable, $Z(s)$, defined by

$$\arg(Z(s)) = \arg(\psi(s, t = 0))$$

and

$$|Z(s)|^2 = \int \mathrm{d}t\, \psi^*(s, t)\hat{j}_s\, \psi(s, t) \tag{1}$$

where $\hat{j}_s$ is the s-component of the current density operator and s increases in the direction

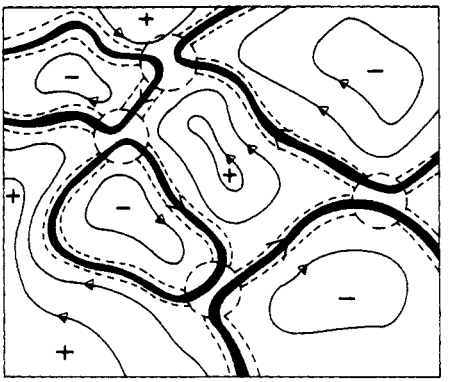

Figure 1. Sketch of a typical potential, $V(x, y)$. Full curves represent equipotentials and arrows give direction of guiding centre motion; + and − denote maxima and minima. Heavy curves indicate contours at potential V_0. Portions of these contours are enclosed in strips and circles (broken lines) which correspond to links and nodes of the network model.

of net current flow on the strip, so the integral is positive. Let Z_i and Z_f be the values of $Z(s)$ at the beginning and end of the strip: since no current flows through the sides of the strip, $Z_f = e^{i\varphi} Z_i$, φ real. The phase, φ, characterises a link of the network model and depends (in a given gauge) on the arc length of the link in units of l_c; we take the φ to be independent random variables uniformly distributed in $[0, 2\pi)$.

Each strip starts and ends at a circle, which encloses a region where two contours approach one another and tunnelling must be considered (the arbitrariness in placing the boundaries of the regions is irrelevant provided $\lambda/l_c \gg 1$). Generically, two incoming and two outgoing strips (defined according to the sense of net current flow) meet at each circle (see figure 2). Let their respective values of $Z(s)$ on the boundary by Z_1, Z_2, Z_3 and Z_4. The result of matching the solution of the Schrödinger equation inside the circle

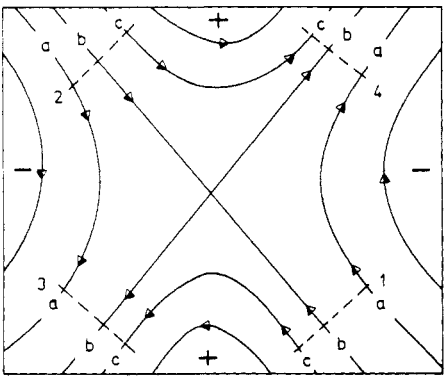

Figure 2. Sketch of a saddle point in the potential, $V(x, y)$. Full curves represent contours and arrows give direction of guiding centre motion. Amplitudes Z_1, Z_2, Z_3 and Z_4 (see text) are defined on the numbered broken lines. Sets of contours labelled (a), (b) and (c) correspond to potentials V_0 which are, respectively, $V_0 \ll V_{00}$, $V_0 \simeq V_{00}$ and $V_0 \gg V_{00}$, where V_{00} is the saddle-point potential.

to the solutions on the four strips can be summarised by

$$\begin{pmatrix} Z_1 \\ Z_3 \end{pmatrix} = \mathbf{M} \begin{pmatrix} Z_4 \\ Z_2 \end{pmatrix}. \tag{2}$$

The 2×2 matrix, $\mathbf{M}$, is constrained by unitarity: we require $|Z_1|^2 + |Z_2|^2 = |Z_3|^2 + |Z_4|^2$ for all Z_2, Z_4. This implies

$$\mathbf{J} = \mathbf{M}^{+}\mathbf{J}\mathbf{M} \tag{3}$$

where

$$\mathbf{J} = \begin{pmatrix} 1 & 0 \\ 0 & -1 \end{pmatrix}$$

which has the general solution

$$\mathbf{M} = \begin{pmatrix} e^{i\varphi_1} & 0 \\ 0 & e^{i\varphi_2} \end{pmatrix} \begin{pmatrix} \cosh\theta & \sinh\theta \\ \sinh\theta & \cosh\theta \end{pmatrix} \begin{pmatrix} e^{i\varphi_3} & 0 \\ 0 & e^{i\varphi_4} \end{pmatrix} \tag{4}$$

with θ, φ real. The φ_i can be set to zero by a choice of gauge, leaving θ to characterise a node of the network model.

In principle, θ could be calculated by solving the Schrödinger equation inside the circle (i.e. near a saddle point of $V(x, y)$), assuming a functional form for the potential in this region. However, the qualitative information we need—how θ depends on V_0—can be obtained much more easily. Referring again to figure 2, let V_{00} be the value of the potential at the saddle point. If $V_0 \ll V_{00}$ (case (a) in figure 2), we expect $|Z_1|^2 \simeq |Z_4|^2$ for almost all values of Z_2 and Z_4, which is the case if $\theta \ll 1$. Conversely, if $V_0 \gg V_{00}$ (case (c)), we expect $|Z_1|^2 \simeq |Z_3|^2$ almost always, which implies $\theta \gg 1$. An intermediate, symmetric value of θ ($V_0 \simeq V_{00}$; case (b)) can be identified by re-writing equation (2) as

$$\begin{pmatrix} Z_1 \\ Z_4 \end{pmatrix} = \mathbf{M}' \begin{pmatrix} Z_3 \\ Z_2 \end{pmatrix}. \tag{5}$$

Naturally, $\mathbf{M}'$ has the form of equation (4); one finds

$$\theta' = \cosh^{-1}(\coth\theta) \equiv f(\theta). \tag{6}$$

The equation $\theta' = \theta$ has the solution $\theta = \theta_c \equiv \ln(1 + \sqrt{2}) \simeq 0.8814$.

A network model that represents a system having a potential, $V(x, y)$, without special correlations will have nodes characterised by a range of θ-values. The median of the distribution will vary with the energy of eigenstates considered, from values much less than θ_c in the low-energy tail of a Landau band to values much greater than θ_c in the high-energy tail. Our main numerical results are for a simplified model in which every node is identical, so as to minimise complications in interpretation arising from crossover between classical percolation and quantum tunnelling regimes. The single value of θ that parameterises this simplified model is an (unknown) monotonic function of energy; because of the symmetry embodied in equation (6) it is necessary to study only one half of the Landau band: $\theta_c \leqslant \theta < \infty$. We assume later that θ can be approximately linearly related to E over a reasonable range in the vicinity of θ_c.

Definition of the network model is completed by describing the interconnections of the elements—links and modes—and the boundary conditions. Realistically, one should study a network that is topologically disordered; instead, we suppose that randomness

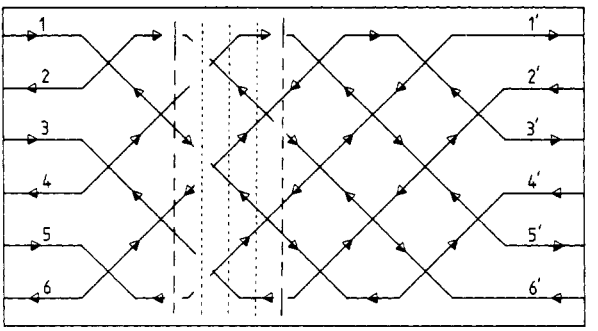

Figure 3. A network with $M = 6$, $N = 4$ and strip boundary conditions, connected to semi-infinite, ideal conductors. Arrows indicate direction of current flow. A 'slice' of the system is contained between broken lines; sub-slices corresponding to the matrices **A**, **B**, **C** and **D** (equation (9)) are contained between broken lines. The transfer matrix relates amplitudes on the links marked $1, 2, \ldots, 6$ to those on the links marked $1', 2', \ldots, 6'$.

in link phases alone is sufficient and study only a square network. The directions of current flow on different links must be related so that there is circulation around each elementary plaquette (see figure 1). Boundary conditions are dictated mainly by the numerical method used: the only efficient simulation technique known is to calculate, not eigenfunctions in a finite system, but transfer matrices for long, narrow samples connected at both ends to semi-infinite, ideal conductors (MacKinnon and Kramer 1981, 1983, Pichard and Sarma 1981). Periodic boundary conditions are applied across the width of the sample (giving a cylinder), to eliminate edge effects; some limited results for the strip geometry have also been obtained.

The above discussion can be summarised, and the network model defined formally, as follows. A complete network is sketched in figure 3. Our aim is to calculate the transfer matrix, **T**, that relates the amplitudes, $\{Z_i\}$, on the left to those, $\{Z_i'\}$, on the right (where $i = 1, 2, \ldots M$, with M even, in a system of width M)

$$Z_i' = T_{ij} Z_j. \tag{7}$$

The network can be cut into slices (each of thickness 2, using the same unit as for width) such as the one contained between broken lines in figure 3. The matrix **T** is the product of transfer matrices $\{\mathbf{U}_\alpha\}$ for each of the N slices

$$\mathbf{T} = \mathbf{U}_1 \mathbf{U}_2 \ldots \mathbf{U}_N. \tag{8}$$

For clarity, we define $\mathbf{U}_\alpha$ as a product of four matrices (corresponding to the four sub-slices between dotted lines in figure 3)

$$\mathbf{U}_\alpha = \mathbf{A}_\alpha \mathbf{B} \mathbf{C}_\alpha \mathbf{D}. \tag{9}$$

Here

$$[A_\alpha]_{ij} = \delta_{ij} \, e^{i\varphi_j(\alpha)} \tag{10}$$

where the $\{\varphi_j(\alpha)\}$ are independent random variables, uniformly distributed in $[0, 2\pi)$; $\mathbf{C}_\alpha$ has an identical form with independent phases. The matrices **B** and **D** are block

diagonal, being composed of 2×2 blocks **M** (equation (4)).

$$\begin{aligned} B_{ii} &= \cosh \theta' && i = 1, 2, \ldots, M \\ B_{2i,2i-1} &= B_{2i-1,2i} = \sinh \theta' && i = 1, \ldots, M/2. \end{aligned} \tag{11}$$

Otherwise $B_{ij} = 0$.

$$\begin{aligned} D_{ii} &= \cosh \theta && i = 2, 3, \ldots, M-1 \\ D_{2i+1,2i} &= D_{2i,2i+1} = \sinh \theta && i = 1, \ldots, M/2 - 1. \end{aligned} \tag{12a}$$

In cylindrical geometry

$$\begin{aligned} D_{11} &= D_{MM} = \cosh \theta \\ D_{1M} &= D_{M1} = \sinh \theta. \end{aligned} \tag{12b}$$

In strip geometry

$$D_{11} = D_{MM} = 1. \tag{12c}$$

Otherwise $D_{ij} = 0$.

The values of θ and θ' in equations (11) and (12) satisfy equation (6). This ensures that the system is invariant (on average) under rotation through 90° (apart from boundary conditions); an anisotropic version of the model, in which θ and θ' are independent

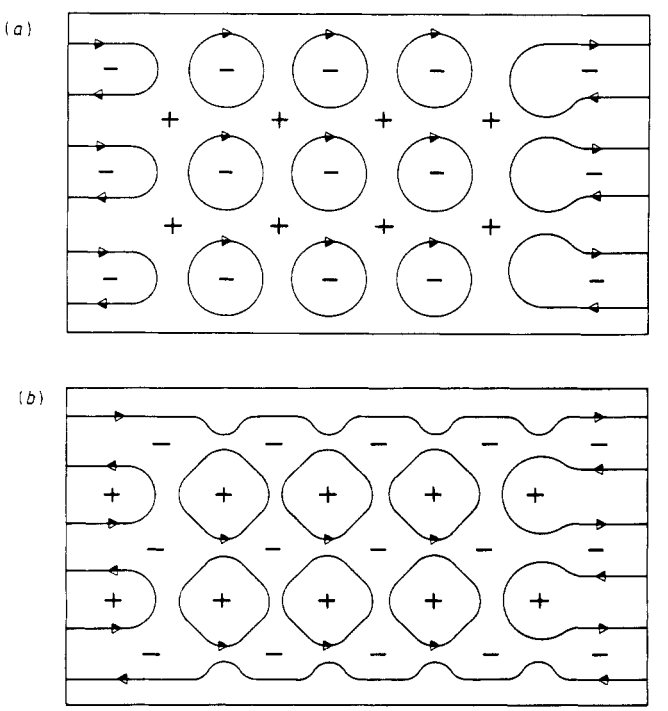

Figure 4. The network of figure 3 reduces to a set of disconnected loops in the tails of the Landau band where quantum tunnelling is negligible and the classical picture is accurate. (*a*) In the low-energy tail, the loops enclose minima in the potential (−); (*b*) in the high-energy tail they enclose maxima (+).

parameters, is also discussed in the following section. This relationship between θ and θ' means that in the extreme lower and upper tails of the Landau band ($\theta = 0$ and $\theta = \infty$), where tunnelling is negligible, the network decomposes into the sets of loops shown in figure 4, as expected from the classical picture. In the first limit, the loops derive from elementary plaquettes of the network around which the current circulation is (say) clockwise: these loops enclose minima in the potential. Correspondingly, in the second limit the loops derive from anticlockwise plaquettes and enclose maxima (obviously, if the magnetic field is reversed, the sense of circulation around each plaquette also reverses).

The transfer matrix approach to localisation has been discussed by many authors; in particular, Anderson (1981) has emphasised that microscopic details of the channels (our links) and scattering between them (our nodes) should be relatively unimportant. This network model is a special case of a more general class of systems (see, for example, Shapiro 1982) in which channels transmit waves in both directions. In the general case, nodes are characterised by a 4×4 S-matrix which relates incident to relfected amplitudes. Our network model has (labelling links as in figure 2)

$$\mathbf{S} = \begin{array}{c} \\ 1 \\ 2 \\ 3 \\ 4 \end{array} \begin{array}{c} \begin{array}{cccc} 1 & 2 & 3 & 4 \end{array} \\ \begin{bmatrix} 0 & 0 & 1/c & -t \\ 0 & 0 & t & 1/c \\ 1/c & -t & 0 & 0 \\ t & 1/c & 0 & 0 \end{bmatrix} \end{array} \tag{13}$$

where $c = \cosh\theta$ and $t = \tanh\theta$. Clearly, the feature that ensures this network model represents the quantum Hall regime is the suppression of propagation in one direction on each link, which is replaced in the formulation based on a 4×4 S-matrix by complete decoupling of the forward and reverse propagating amplitudes.

A network model without disorder in the link phases was derived and studied some years ago by Pippard (1964), who was concerned with magnetic breakdown in the de Haas–van Alphen effect. Tunnelling in that case occurs in k-space, but the mathematical description is the same.

3. Calculation and results

Our numerical calculation follows the methods of previous authors (MacKinnon and Kramer 1981, 1983, Pichard and Sarma 1981, see also Benettin *et al* 1980). Let the eigenvalues of $\mathbf{T}^{+}\mathbf{T}$ for a system of length N 'slices' be $\{\gamma_i(N)\}$, $\gamma_1(N) \geqslant \gamma_2(N) \geqslant \ldots \geqslant \gamma_M(N)$. Effectively, we calculate

$$\xi_M(\theta) \equiv [(1/4N)\ln(\gamma_{M/2}(N))]^{-1} \tag{14}$$

for large N, which is identified with the localisation length in a quasi one-dimensional system of width M. (The factor of 4 appearing in (14) makes the units of ξ and M the same.)

The largest systems studied were of width $M = 128$ and length $N = 10^5$, which required the same computational effort as a tight-binding model with $M = 64$, $N = 10^5$ and complex, nearest-neighbour hopping elements. For $M = 128$ we estimate (following MacKinnon and Kramer 1983) that the localisation length was determined with an

accuracy of ±2%; in narrower systems ($M = 64, 32, 16, 8$ and 4) the estimated accuracy is ±1%.

An initial impression of the results is given by the behaviour of the renormalised localisation length

$$\Lambda_M(\theta) = \xi_M(\theta)/M \tag{15}$$

as a function of θ, or, equivalently, energy in the Landau band, for increasing system width. If eigenstates are extended at a given value of θ, one expects $\xi_M(\theta)$ to increase at least linearly with M, so that $\Lambda_M(\theta)$ is constant or an increasing function of M. Conversely, if eigenstates are localised, so that $\xi_\infty(\theta)$ is finite, one expects $\xi_M(\theta)$ to saturate when $M \gg \xi_\infty(\theta)$, so that $\Lambda_M(\theta)$ is a decreasing function of M, given asymptotically for M large by $\xi_\infty(\theta)/M$. We find (figure 5) at the Landau band centre ($\theta = \theta_c$) that $\Lambda_M(\theta)$ is independent of M, indicating extended eigenstates, whilst in the band tail there is clear evidence that eigenstates are localised. A numerical simulation cannot, of course, demonstrate conclusively that eigenstates are extended only at one energy in the Landau band, but it is apparent from the data for the widest systems that states are localised even very close to the band centre. If there is a mobility edge at

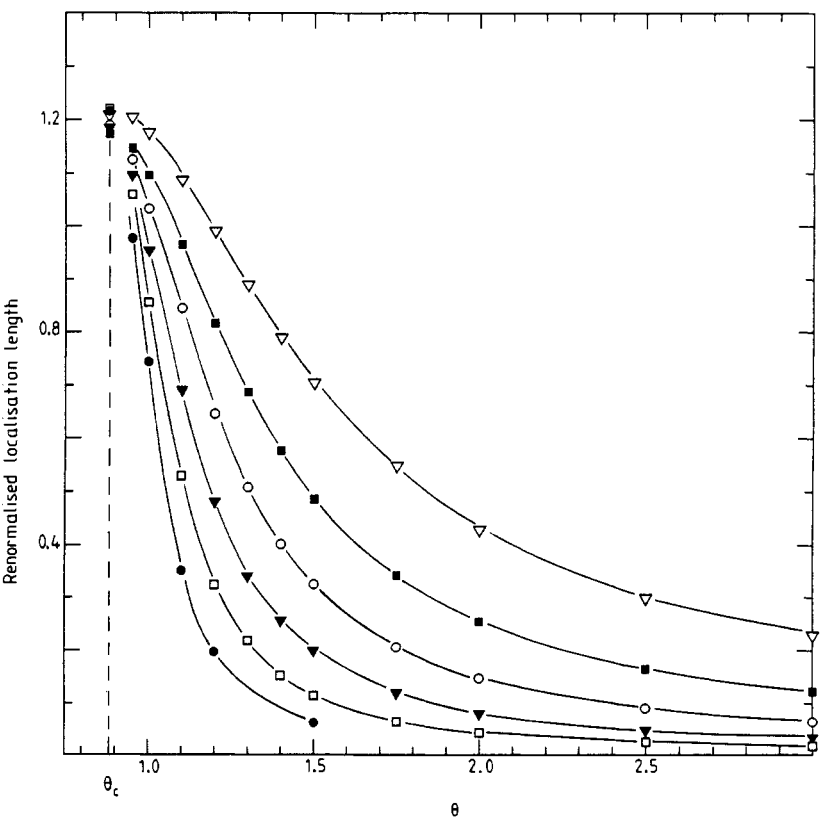

Figure 5. The renormalised localisation length, $\Lambda_M(\theta)$, as a function of θ (or energy), from the Landau band centre to the upper band tail, for systems of widths: $M = 4$ (▽); $M = 8$ (■); $M = 16$ (○); $M = 32$ (▼); $M = 64$ (□) and $M = 128$ (●). The vertical broken line marks the Landau band centre.

parameter value θ_μ distinct from θ_c, then $(\theta_\mu - \theta_c)/\theta_c < 0.05$; there is no obvious aspect of the network model that might set such a small scale.

More detailed information is given by a scaling analysis of the data. If the localisation length on cylinders satisfies one-parameter scaling (there are actually reasons for expecting it not to: see below), then $\Lambda_M(\theta)$, instead of depending separately on M and θ, obeys

$$\Lambda_M(\theta) = g(\xi_\infty(\theta)/M). \tag{16}$$

The results of fitting our data in this way (approximating $\log(g(x))$ with a sixth-order polynominal in $\log(x)$) are shown in figures 6 and 7. The collapse of all data onto one curve, $g(x)$, in figure 6 is striking. The deviations that do occur are mainly in the narrowest systems, for which finite-size corrections to equation (16) might be expected: χ^2 per data point decreases from 8 to 3 if results for $M = 4$ are excluded. This strong evidence for one-parameter scaling in the network model is remarkable in view of the expectation (Kheml'nitzkii 1983, Wei *et al* 1986) that, in general, a two-parameter scaling theory is necessary to describe the quantum Hall effect. Our results can only be reconciled with the proposed flow diagram given in figure 1 of Khmel'nitzkii (1983), if the short-distance

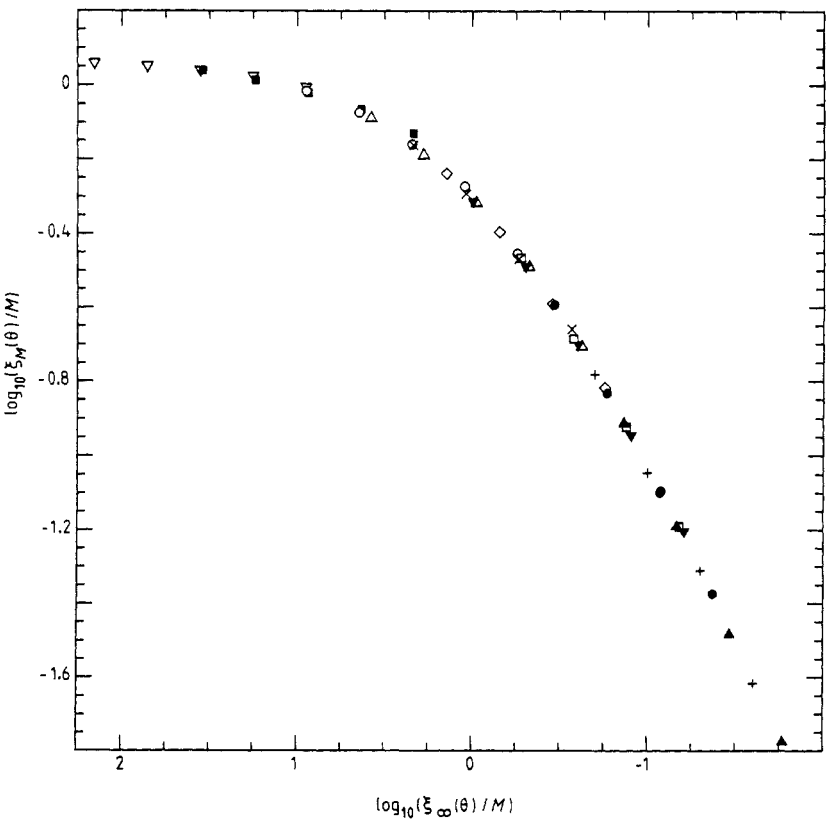

Figure 6. A fit of the data shown in figure 5 to a one-parameter scaling form: $\log_{10}(\Lambda_M(\theta))$ versus $\log_{10}(\xi_\infty(\theta)/M)$. Symbols denote parameter values $\theta = 0.95$ (▽); $\theta = 1.0$ (■); $\theta = 1.1$ (○); $\theta = 1.2$ (△); $\theta = 1.3$ (×); $\theta = 1.4$ (◇); $\theta = 1.5$ (▼); $\theta = 1.75$ (□); $\theta = 2.0$ (●); $\theta = 2.5$ (+) and $\theta = 3.0$ (▲).

properties of the network model happen to place it on the flow line connecting the localised and extended fixed points, for all values of the parameter θ. We do not know whether this is plausible or not.

Ando and Aoki (1985) have examined the effect of varying λ/l_c using finite-size scaling in the lowest Landau level; they find that breakdown of one-parameter scaling becomes more pronounced as λ/l_c increases. (We are grateful to a referee for emphasising this point.) A possible explanation is that scaling flow in their model is complicated by crossover from classical percolation to quantum localisation fixed points. It seems reasonable that the system they study should initially have the same scaling behaviour as in classical percolation, if λ/l_c is large. Contrastingly, the network model is designed not to do this, since the tunnelling parameters are chosen to be the same at each node.

Scaling analysis also yields the dependence of the localisation length in an infinite system, $\xi_\infty(\theta)$, on θ, or energy (figure 7). The result is consistent with a divergence at

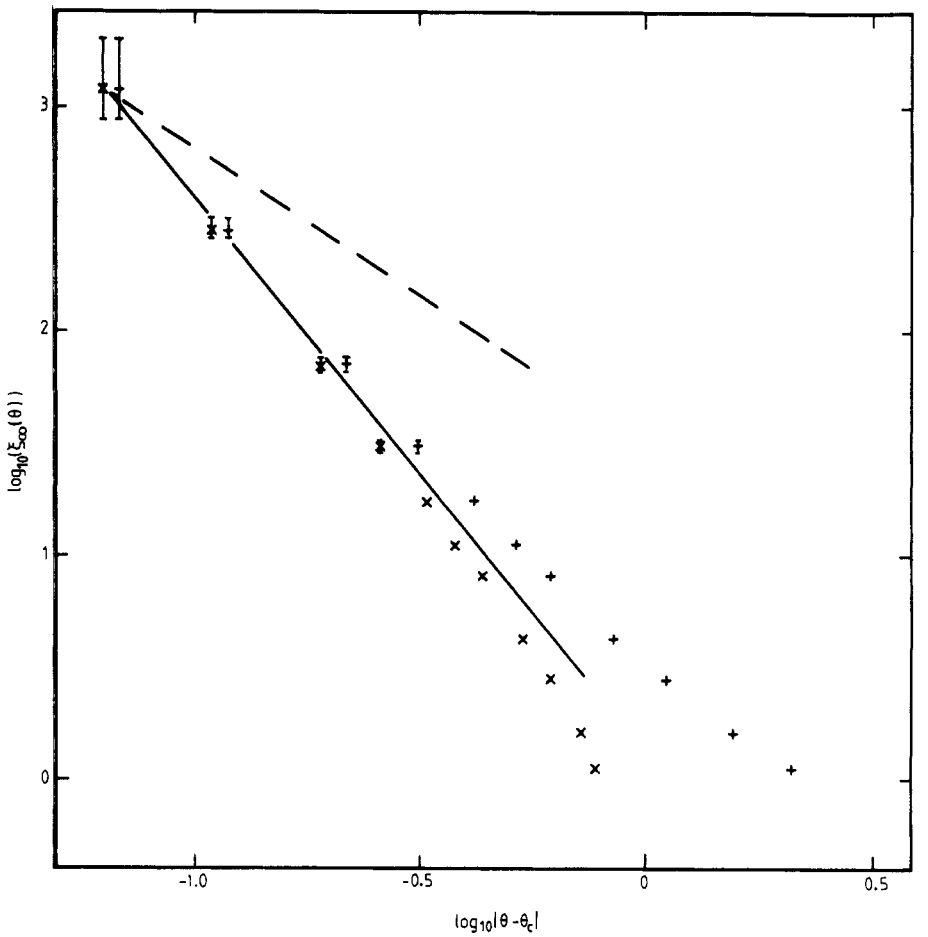

Figure 7. Dependence of localisation length on energy: $\log_{10}(\xi_\infty(\theta))$ (the fitting parameters obtained from figure 6) versus $\log_{10}|\theta - \theta_c|$. The upper right set of points are for $\theta > \theta_c$; the lower left set are for $\theta < \theta_c$. The two sets are asymptotically coincident as $|\theta - \theta_c| \to 0$. The full line has slope $\nu = 2.5$; the broken line corresponds to the classical percolation value: $\nu = \frac{4}{3}$. Estimated uncertainties in $\xi_\infty(\theta)$ are represented by vertical error bars.

the band centre of the form $\xi_\infty(\theta) \sim A|\theta - \theta_c|^{-\nu}$ for $|\theta - \theta_c|$ small, with $A = 1.3 \pm 0.1$ and $\nu = 2.5 \pm 0.5$. This value for the correlation length exponent is quite different to $\nu = \frac{1}{2}$, obtained by Affleck (1986) from a field-theoretic representation (Levine *et al* 1983) of a system with an uncorrelated potential. It is probably also distinct from the value $\nu = \frac{4}{3}$ resulting from the classical percolation picture (Trugman 1983), which demonstrates the relevance of quantum tunnelling and interference effects near the percolation threshold. Our value is consistent with the Harris condition, $\nu > 1$ in two-dimensional systems (Chayes *et al* 1986). Interestingly, it is in reasonable agreement with two numerical estimates for the lowest Landau level with an uncorrelated potential: Aoki and Ando (1985) obtained $\nu \geqslant 2$ using finite-size scaling; Hikami (1986) found $\nu = 1.9 \pm 0.2$ by analysing a perturbation series in powers of the potential. This suggests that inclusion of quantum tunnelling causes crossover from classical percolation to universal quantum critical behaviour.

There is a general amplitude exponent relationship that is valid in finite-size scaling on cylinders for systems at a conformally invariant critical point (Cardy 1984, 1987; for a heuristic derivation, directly applied to localisation, see Pichard and Sarma (1981)). In the present context, the consequence is that if eigenfunctions, $\psi(\boldsymbol{r})$, have correlations that are conformally invariant at the mobility edge, then the amplitude, a, defined by $\xi_M(\theta_c) = aM$ is related to the exponent, η, defined by $|\psi(\boldsymbol{r})\psi(\boldsymbol{r}')| \sim |\boldsymbol{r} - \boldsymbol{r}'|^{-\eta}$ for large $|\boldsymbol{r} - \boldsymbol{r}'|$ according to

$$\eta = 1/\pi a. \tag{17}$$

Under this assumption, we find $\eta = 0.269 \pm 0.003$. A positive value for η is consistent with a general inequality for eigenfunction correlations in a single Landau level (Chalker 1987); the conflict with the result $\eta = 2 - d$ (Wegner 1976), derived from the requirement of homogeneity under combined energy and length scale transformations, will be discussed elsewhere (Chalker 1988).

A test of conformal invariance in this and other models for localisation would be very desirable. We have been able to examine a limited aspect by simulating an anisotropic version of the network model. In this version, θ and θ' (equations (11) and (12)) are independent parameters, no longer related via equation (6), so the system is not invariant under 90° rotations. In the infinite system, if states are localised, anisotropy has the effect that there are two different localisation lengths associated with the two directions of diagonals on the network. One localisation length, $\xi_\infty(\theta, \theta')$, is obtained by studying cylinders with the chosen values of θ and θ'; the other, $\bar{\xi}_\infty(\theta, \theta')$, is calculated (see the discussion preceding equation (6)) by replacing θ with $f(\theta)$ and θ' with $f(\theta')$. The two localisation lengths are related by

$$\bar{\xi}_\infty(\theta, \theta') = \xi_\infty(f(\theta), f(\theta')). \tag{18}$$

The phase diagram of the anisotropic model in the (θ, θ') plane appears to be very simple: both lengths are divergent on the line $\theta = \theta'$, and finite elsewhere. Evidence for this is summarised in figure 8, in which contours of the ratio

$$r_M = \xi_{2M}(\theta, \theta')/\xi_M(\theta, \theta') \tag{19}$$

are drawn on (θ, θ') for $M = 8$. We expect $r_\infty \geqslant 2$ where states are extended, and $r_\infty = 1$ where states are localised. In practice, finite-size effects are large at $M = 8$, but experience with the isotropic model indicates that values of $r_M < 2$ scale towards $r_\infty = 1$ with increasing M.

The relevance of the anisotropic model as a test of a prediction from conformal

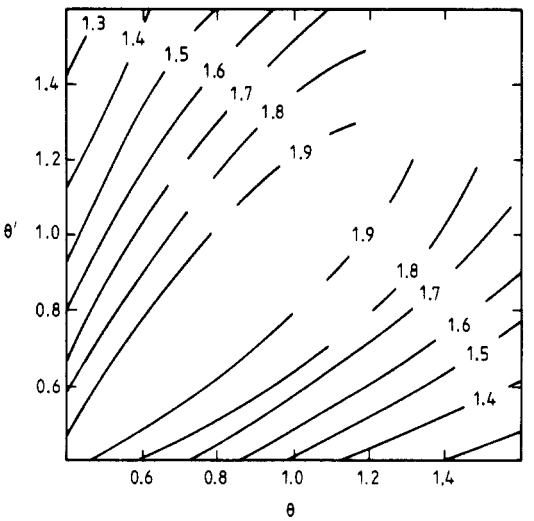

Figure 8. The position of the mobility edge in the anisotropic model. Contours of the ratio r_M (see equation (19)) drawn in the θ–θ' plane for $M = 8$. States are probably extended ($r_\infty = 2$) on the line $\theta = \theta'$ and localised ($r_\infty = 1$) elsewhere.

invariance is the following. On the critical line, $\theta = \theta'$, amplitudes $a(\theta)$ and $\bar{a}(\theta)$ can be derived from $\xi_M(\theta, \theta)$ and $\bar{\xi}_M(\theta, \theta)$ as before. If correlations are conformally invariant after an appropriate relative scaling of lengths in the two directions, and also independent of θ, one expects (Cardy 1987) that the value of η determined using the geometric mean of the amplitudes, $(a(\theta)\,\bar{a}(\theta))^{1/2}$, should not depend on θ. Results in table 1 demonstrate that variations in this mean are much smaller than variations in $a(\theta)$ or $\bar{a}(\theta)$ separately.

Table 1. Localisation length amplitudes along the critical line of the anisotropic model (see text). Variations in $(a(\theta)\,\bar{a}(\theta))^{1/2}$ are much smaller than those in $a(\theta)$ or $\bar{a}(\theta)$ separately.

θ	$a(\theta)$	$\bar{a}(\theta)$	$(a(\theta)\,\bar{a}(\theta))^{1/2}$
0.8814	1.18 ± 0.01	1.18 ± 0.01	1.18 ± 0.01
0.8	1.45 ± 0.02	0.929 ± 0.01	1.16 ± 0.01
0.6	2.83 ± 0.03	0.473 ± 0.003	1.16 ± 0.01

We have also studied a second modification of the original system, in order to find the effect of free boundaries: cylindrical geometry was replaced by strip geometry (see equation (12)), with an isotropic choice for θ and θ'. In this case, for values of θ (energies) above the Landau band centre, the longest localisation length rapidly becomes unmeasurably large with increasing strip width; the next longest localisation length, derived from $\gamma_{M/2-1}$, behaves much as the longest length in cylindrical geometry. Below the band centre, the longest localisation length is not much affected by boundary conditions, in wide strips. We interpret this to indicate that there are extended edge states on the strip at all energies above the Landau band centre, and that the bulk

transition is unaffected by boundary conditions. Similar results were obtained by Schweitzer *et al* (1984) with a lattice model. For brevity we omit data.

4. Summary

A network model for localisation in the integer quantum Hall regime has been introduced which makes possible numerical simulation of a system in which the disorder potential varies slowly on the magnetic length scale. Results are broadly compatible with earlier simulations of models with an uncorrelated potential (Schweitzer *et al* 1984, Aoki and Ando 1985), indicating extended states probably at only one energy in each Landau band. The scaling behaviour of the network model is, however, surprisingly simple, being well represented by a one- (rather than two-) parameter scaling function. The value of the localisation length exponent is compatible with numerical results for an uncorrelated potential and suggests that quantum tunnelling induces universal quantum critical behaviour at the classical percolation threshold. If correlations at the mobility edge are conformally invariant, then eigenfunctions have power-law decay. The model demonstrates that the localisation behaviour implied by observations of the integer quantum Hall effect can be generated from remarkably few ingredients.

Acknowledgments

The numerical calculations were done using a Meiko Computing Surface containing 32 Inmos T414 transputers. We particularly wish to thank B D Carpenter for technical advice and A J G Hey for encouragement. One of us (JTC) is also grateful for fruitful discussions with G J Daniell, J M F Gunn (who drew attention to the work by Pippard), A MacKinnon and B Shapiro (who clarified the relationship between the network model and more general systems). This work was supported in part by the SERC.

References

Affleck I 1986 *Nucl. Phys.* B **265** 409–77
Anderson P W 1981 *Phys. Rev.* B **23** 4828–36
Ando T and Aoki H 1985 *J. Phys. Soc. Japan* **54** 2239–49
Aoki H and Ando T 1985 *Phys. Rev. Lett.* **54** 831–4
Avron J E, Raveh A and Zur B 1987 *Phys. Rev. Lett.* **58** 2110–3
Benettin G, Galgani L, Giorgilli A and Strelcy J-M 1980 *Meccanica* **15** 9–30
Cardy J L 1984 *J. Phys. A: Math. Gen.* **17** L385–7
—— 1987 *Phase Transitions and Critical Phenomena* vol 11, ed. C Domb and J L Lebowitz (New York: Academic) pp 55–126
Chalker J T 1987 *J. Phys. C: Solid State Phys.* **20** L493–8
—— 1988 *J. Phys. C: Solid State Phys.* **21** L119–21
Chalker J T and Siak S 1988 in preparation
Chayes J T, Chayes L, Fisher D S and Spencer T 1986 *Phys. Rev. Lett.* **57** 2999–3002
de Gennes P-G 1981 *C. R. Acad. Sci., Paris C* **292** 9–12, 279–82
Hikami S 1986 *Prog. Theor. Phys.* **76** 1210–21
Iordansky S V 1982 *Solid State Commun.* **43** 1–3
Johnston R J and Kunz H 1983 *J. Phys. C: Solid State Phys.* **16** 3895–912
Kazarinov R F and Luryi S 1982 *Phys. Rev.* B **25** 7626–30
Khmel'nitzkii D E 1983 *JETP Lett.* **38** 552–6

Levine H, Libby S B and Pruisken A M M 1983 *Phys. Rev. Lett.* **51** 1915–7
MacKinnon A and Kramer B 1981 *Phys. Rev. Lett.* **47** 1546–9
—— 1983 *Z. Phys.* B **53** 1–13
Ono Y 1982 *Anderson Localisation* ed. Y Nagaoka and H Fukuyama (Berlin: Springer) pp 207–15
Pichard J L and Sarma G 1981 *J. Phys. C: Solid State Phys.* **14** L127–32, L617–25
Pippard A B 1964 *Phil. Trans. R. Soc.* **256** 317–55
Prange R E and Joynt R 1982 *Phys. Rev.* B **25** 2943–6
Schweitzer L, Kramer B and MacKinnon A 1984 *J. Phys. C: Solid State Phys.* **17** 4111–25
Shapiro B 1982 *Phys. Rev. Lett.* **48** 823–5
—— 1986 *Phys. Rev.* B **33** 8447–57
Trugman S A 1983 *Phys. Rev.* B **27** 7539–46
Tsukada M 1976 *J. Phys. Soc. Japan* **41** 1466–72
von Klitzing K, Dorda G and Pepper M 1980 *Phys. Rev. Lett.* **45** 494–7
—— 1986 *Rev. Mod. Phys.* **58** 519–31
Wegner F 1976 *Z. Phys.* B **25** 327–37
Wei H P, Tsui D C and Pruisken A M M 1986 *Phys. Rev.* B **33** 1488–91
Wilkinson M 1987 *J. Phys. A: Math. Gen.* **20** 1761–71